

Received: 2015.08.13
Accepted: 2015.10.01
Published: 2016.05.31

Identification of Preferentially Expressed Antigen of Melanoma as a Potential Tumor Suppressor in Lung Adenocarcinoma

Authors' Contribution:
Study Design A
Data Collection B
Statistical Analysis C
Data Interpretation D
Manuscript Preparation E
Literature Search F
Funds Collection G

C 1 **Quan Huang***
E 1 **Lin Li***
D 1 **Zaijun Lin***
F 1 **Wei Xu***
EF 1 **Shuai Han**
B 1 **Chenglong Zhao**
AF 1 **Lei Li**
DE 2 **Wenjiao Cao**
CD 1 **Xinghai Yang**
D 1 **Haifeng Wei**
G 1 **Jianru Xiao**

1 Department of Orthopedic Oncology, Changzheng Hospital, The Second Military Medical University, Shanghai, P.R. China
2 The International Peace Maternity & Child Health Hospital of China Welfare Institute (IPMCH), Shanghai, P.R. China

* These authors contributed equally to this work

Corresponding Authors: Jianru Xiao, Haifeng Wei and Xinghai Yang, e-mail: xiaojianru_sh@163.com
Source of support: Departmental sources

Background: Preferentially expressed antigen of melanoma (PRAME) is known as a tumor-associated antigen that is altered in a variety of malignancies, including lung cancer. However, the role of PRAME in lung cancer remains unclear.

Material/Methods: We analyzed the expression of PRAME in human lung adenocarcinomas and studied the function of PRAME using small interfering RNA (siRNA)-induced gene knockdown in lung cancer cell lines PC9 and A549.

Results: We found that PRAME expression is down-regulated in lung adenocarcinomas. Knockdown of PRAME promoted proliferation and suppressed apoptosis of PC9 and A549 cells.

Conclusions: In line with its roles in controlling cell growth, PRAME regulates multiple critical cell-growth related genes, including IGF1R oncogene. IGF1R up-regulation contributes to increase of cell growth upon the knockdown of PRAME. Taken together, our results suggest that PRAME has inhibitory roles in lung cancer.

MeSH Keywords: **Apoptosis • Cell Proliferation • Lung Diseases**

Full-text PDF: <http://www.medscimonit.com/abstract/index/idArt/895642>



2173



—



5



22



Background

Preferentially expressed antigen of melanoma (PRAME) was initially identified as a tumor-associated antigen recognized by cytotoxic T lymphocytes against a melanoma surface antigen [1]. This antigen belongs to the cancer-testis antigens, all of which are absent in normal tissues, but are detected in cancers, including melanoma, breast cancer, lung carcinoma, renal cell carcinoma, and leukemia. Unlike other cancer-testis antigens, PRAME shows some expression in normal tissues, such as testis, ovary, and adrenal gland [1]. PRAME has emerged as a marker of disease activity and prognosis in acute promyelocytic leukemia, primary osteosarcoma, and head and neck squamous cell carcinoma [2,3]. In most cases, the high expression of PRAME has been linked to poor prognosis and increased development of metastasis [4,5]. However, high expression of PRAME in childhood acute myeloid leukemia is a marker of favorable prognosis and longer survival [6].

It has been reported that PRAME inhibits myeloid differentiation in certain myeloid leukemias. It has been shown that over-expression of PRAME blocks retinoid acid receptor-mediated differentiation of normal hematopoietic and leukemic progenitor cells [7]. Knockdown of PRAME inhibits proliferation and causes cell cycle arrest and apoptosis in leukemia cells [8]. These studies indicate PRAME plays important roles in regulating cell proliferation and differentiation. Retinoic acid receptor signaling has been shown to mediate the effect of PRAME. It has been shown that PRAME can bind to the retinoic acid receptors and inhibit the target gene transcription, such as the tumor necrosis factor-related apoptosis-inducing ligand (TRAIL), leading to the inhibition cell differentiation [9,10]. PRAME has also been found in lung cancers [11], but its role in lung cancer cells remains elusive.

In our present study, we demonstrate that knockdown of PRAME increased the proliferation of lung cancer cell lines PC9 and A549. It was further revealed that the apoptosis of lung cancer cells was decreased when PRAME was inhibited. Gene expressions were also analyzed using quantitative RT-PCR in lung cancer cells after PRAME siRNA transfection.

Material and Methods

Histological staining

Lung tissues of 20 normal controls and tumor tissues from 4 lung cancer patients were collected and sectioned. The paraffin sections were dried in an oven at 65°C for 1 h. The paraffin sections were then dewaxed in xylene and rehydrated in a series of ethanol solutions. The endogenous peroxidase activity was blocked through a 10-min pre-incubation with 3% H₂O₂. The

paraffin sections were preheated at 100°C in antigen retrieval solution containing EDTA (pH 8.0) for 30 min and blocked by non-immune goat serum at room temperature for 15 min to decrease unspecific staining. The incubation with mouse polyclonal anti-PRAME (1:1000) was performed overnight at 4°C. After being washed 3 times with 1×PBS buffer for 3 min, the sections were incubated with the second (link) antibody (biotinylated mouse-anti-human IgG) for 30 min at room temperature. After reacting with the streptavidin-biotin-peroxidase complex for 20 min, the immune-reactivity was determined by 3,3'-diamino-benzidinetetrahydrochloride and H₂O₂ at room temperature according to the manufacturer's instructions. A positive reaction was manifested as a brown (DAB) stain. The sections were counterstained in Mayer's hematoxylin. The selected sections were scanned at 400× magnification to visualize the localization and distribution of PRAME (PRAME antibody: SC-6704).

Cell culture and siRNA transfection

PC9 and A549 cells were cultured in RPMI and MEM, both of which were supplemented with 10% fetal bovine serum (FBS), 2 mmol/L glutamine, 100 units/mL penicillin, and 100 µg/mL streptomycin. Cells were cultured in a humidified atmosphere of 95% air and 5% CO₂ at 37°C. For transfection of siRNA, Lipofectamine[®] RNAiMAX Reagent (Invitrogen) was mixed with the siRNA construct according to the manufacturer's instructions and added to PC9 or A549 cells in a 24-well plate. Pre-designed SMARTpool ON-TARGET plus PRAME siRNA duplexes were designed and synthesized by Dharmacon (Lafayette, CO).

Quantitative reverse transcriptase-polymerase chain reaction (qRT-PCR)

The total RNAs from PC9 or A549 cells were prepared using the TRIzol reagent (Invitrogen, Carlsbad, CA). One µg of total RNAs was treated with DNase I (Invitrogen) and the cDNA was synthesized *in vitro* from the mRNA template using SuperScript[®] III First-Strand Synthesis Kit (Invitrogen). We used 18s rRNA as the internal control. The mRNA expression levels of target genes were determined by quantitative real-time PCR by using SYBR Green (Applied Biosystems) and normalized to that of 18s rRNA in each group using the equation: $2^{-(CT_{18s} - CT_{PRAME \text{ or other target genes}})}$, where CT is the threshold cycle for each gene [12].

The sequences of primers are as follows:

PRAME forward primer 5-CAGGACTTCTGGACTGTATGGT-3;
PRAME reverse primer 5-CTACGAGCACCTCTACTGGAA-3;
β-actin forward primer 5- CGTCATACTCCTGCTTGCTG-3;
β-actin reverse primer 5- GTACGCCAACACAGTGCTG-3;
BNIP3 forward primer 5-CAGGGCTCCTGGGTAGAACT -3;
BNIP3 reverse primer 5- CTACTCCGTCCAGACTCATGC-3;
DAPK1 forward primer 5-GAGTTTGTGCTCCTGAGATAGT-3;

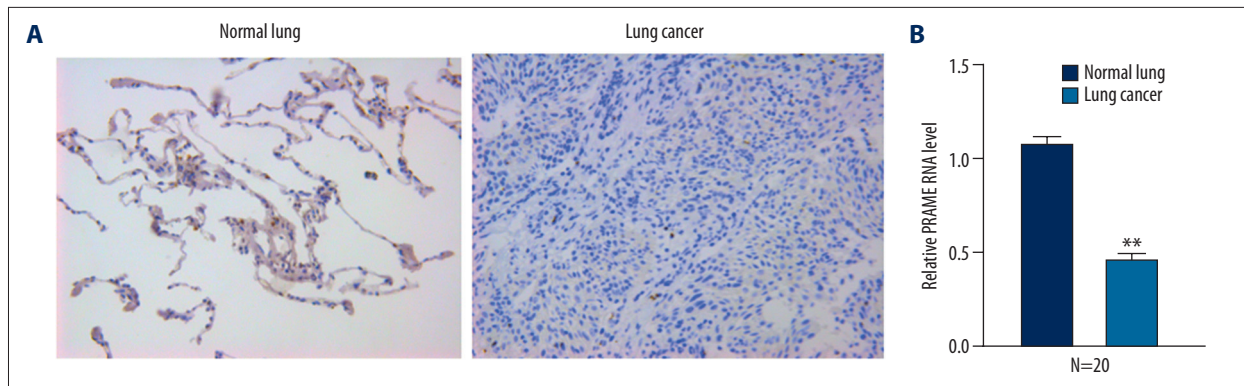


Figure 1. Expression of PRAME in normal human lung and human lung adenocarcinoma. (A) Immunohistochemical staining shows that PRAME immunoreaction is detected in normal human lung tissue and human lung adenocarcinoma (right). (B) The expression of PRAME was also measured using RT-PCR assay. * $p < 0.05$ compared between 2 groups.

DAPK1 reverse primer 5- GCTTAGTGTCTCCAAGAAATGGG.-3;
p21 forward primer 5-TGTCCTCAGAACCCATGC -3;
p21 reverse primer 5- AAAGTCGAAGTTCATCGCTC-3;
BCL10 forward primer 5-TCTGGACACCTTGTGAATCT -3;
BCL10 reverse primer 5- TGGAAAAGGTTACAACCTGCTAC-3;
BNIP3L forward primer 5-TTGATGCACAACATGAATCAGG -3;
BNIP3L reverse primer 5-TCTTCTGACTGAGAGCTATGGTC -3;
CASP8 forward primer 5-TCATGGACCACAGTAACATGGA -3;
CASP8 reverse primer 5- AGTGAAGTGTGATGTCAGTCTCAT.-3;
CASP10 forward primer 5-AGAACTGCTCTACGAAGTGT -3;
CASP10 reverse primer 5-GGGAAGCGAGTCTTTCAGAAG-3;
IGF1R forward primer 5-ATGCTGACTCTGTACCTCT -3;
IGF1R reverse primer 5-GGCTATTCCCACAATGTAGTT -3;

MTT assay

PC9 and A549 cells were seeded in 96-well microplates with 2000 cells/well and incubated for 24 h in 100 μ l culture medium. The cells were then treated with control or PRAME siRNA for 48 h. MTT was added to the cells, which were then cultivated for another 4 h. Following the removal of the supernatant, DMSO (100 μ l/well) was added to the cells, which were agitated for 15 min. The absorbance (OD) was measured at 570 nm by an ELISA reader. Each assay was repeated 3 times [13].

Apoptosis analysis with flow cytometry

Cell apoptosis was determined by use of the Annexin V-FITC/PI Apoptosis Detection Kit (Abcam, Cambridge, MA, USA) according to the manufacturer's protocols using flow cytometry. After control and PRAME siRNA treatments, the cells were harvested, washed 2 times with pre-chilled PBS and resuspended in 1X binding buffer at a concentration of 1×10^6 cells/ml. This solution (100 μ l) was mixed with 5 μ l annexin V-FITC and 5 μ l PI for 15 min, then 400 μ l 1X binding buffer was added. The analysis was carried out using a FACStar cytofluorometer with CXP software.

Western blot

Whole-cell lysates from PC9 and A549 cells were prepared and separated using 10% SDS-PAGE gel. After blocking with Tris-buffered saline/0.05% Tween 20 containing 5% skim milk or 3% bovine serum albumin (Sigma, St. Louis, MO), blots were incubated at 4°C overnight with the primary antibodies against human PRAME protein (1:200), p27 (1:500), cleaved caspase-8 (1:200), IGF1R (1:200), and actin (1:5000), respectively. Horseradish peroxidase conjugated IgG was used as secondary antibody according to the manufacturer's instructions.

Statistical analysis

Data are presented as mean \pm SEM of 3 independent experiments. Significance of means between 2 groups was determined by *t* test. Difference in cell growth between control and PRAME siRNA-treated groups was evaluated by repeated measures analysis of variance (ANOVA). A P-value of < 0.05 was considered significantly different.

Results

PRAME expression is down-regulated in lung carcinoma

To study the role of PRAME in lung cancer cells, we examined the expression of PRAME in normal human lung tissue and in human lung adenocarcinoma. Immunohistochemical staining shows that PRAME is expressed in both normal lung and lung cancer tissues. As shown in Figure 1, the PRAME immunoreactivity in the normal lung tissue was stronger than that in the human lung adenocarcinoma. The mRNA expression of PRAME was also examined in both tissues using RT-PCR studies. Consistent with the immunohistochemical study, the mRNA expression of PRAME in lung cancer tissue was significantly lower than that in normal lung tissue.

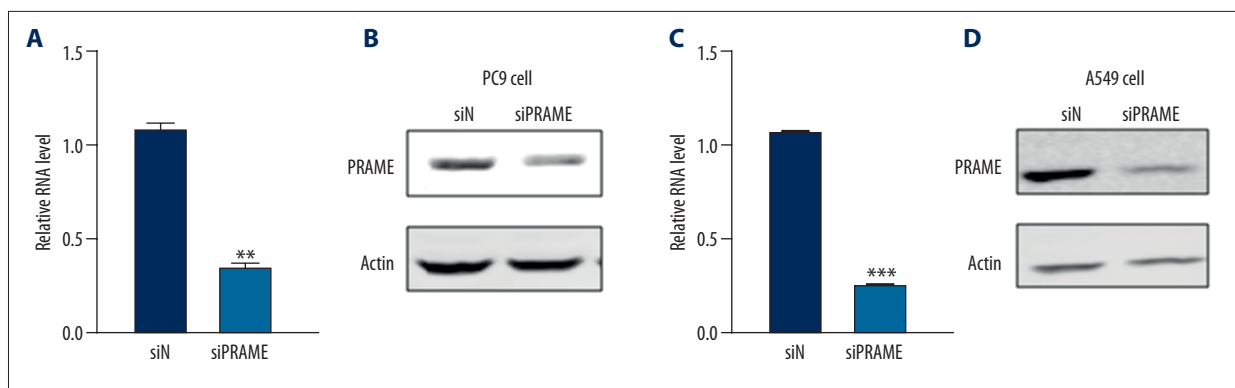


Figure 2. Changes in PRAME expression after siRNA transfection. Messenger RNA (A) and protein expression (B) are decreased in PC9 cells transfected with PRAME siRNA (siPRAME) compared with that in control siRNA-treated group (siN). Messenger RNA (C) and protein expression (D) are decreased in A549 cells transfected with PRAME siRNA (siPRAME). Actin serves as the loading control in the experiments. * $p < 0.05$.

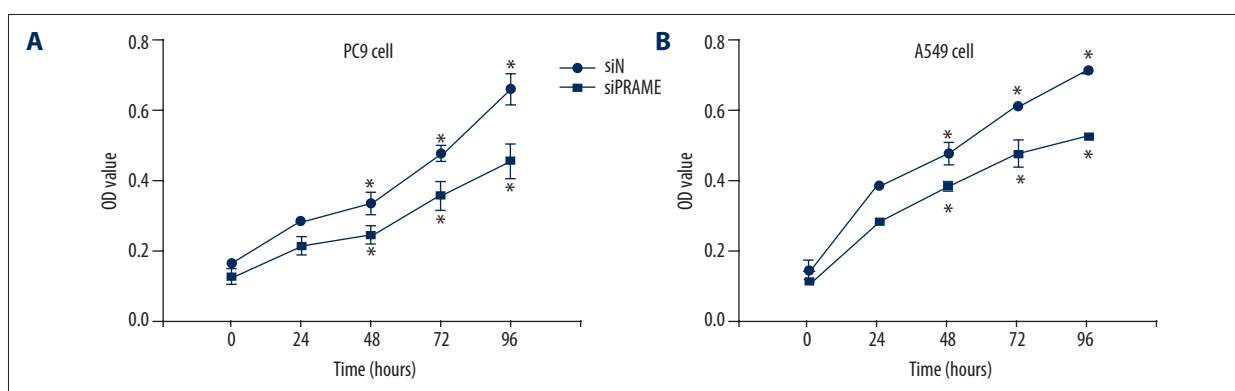


Figure 3. Cell proliferation of PRAME siRNA-treated cells. MTT assay of PC9 cells (A) and A549 cells (B) after PRAME (siPRAME) and control siRNA (siN) transfection. * $p < 0.05$.

Inhibition of PRAME promotes lung cancer cell proliferation

Next, we knocked down the expression of PRAME in lung cancer cells using siRNA technique. As shown in Figure 2, 2 days after the PRAME siRNA transfection, the PRAME mRNA expression was significantly reduced in PC9 and A549 cells compared with control siRNA-transfected cells. The Western blot analysis demonstrated that PRAME protein expression was also dramatically inhibited after siRNA transfection. It was further revealed that after the PRAME siRNA transfection, the cell proliferation of lung cancer cells PC9 and A549 was increased, as evidenced by the increased cell growth 48 h after transfection measured by the MTT assay (Figure 3). The increased cell proliferation was observed between day 2 and day 4 compared with control siRNA-treated cells.

Inhibition of PRAME inhibits lung cancer cell apoptosis

To further examine the effect of PRAME on cell growth, cell apoptosis was analyzed using flow cytometry. As shown in Figure 4,

PRAME knockdown in PC9 cells led to a significant decrease of the percentage of annexin V-positive fractions, with the early apoptotic cells decreased from 7.87% to 1.42% and late apoptotic cells decreased from 6.7% to 4.85%. Consistent with the flow cytometry data, a decreased level of cleaved caspase-8 was also detected in cells treated with PRAME siRNA, suggesting the inhibition of apoptosis induced by PRAME knockdown.

PRAME regulates critical cell-growth related genes, including IGF1R oncogene

We asked which genes might be responsible for the effects of PRAME on cell proliferation and apoptosis. In order to identify potential candidate genes, we performed a quantitative RT-PCR analysis and compared the gene expression profile of lung cancer cells transfected with PRAME siRNA with that treated with control siRNA. We found that several genes are down-regulated, including BNIP3, DAPK1, p21, BCL10, CASP8, CASP10, and BNIP3L (Figure 5A), which cause cell cycle arrest, inhibit proliferation, and promote apoptosis. On the other hand, both the mRNA and protein expression of insulin-like growth factor

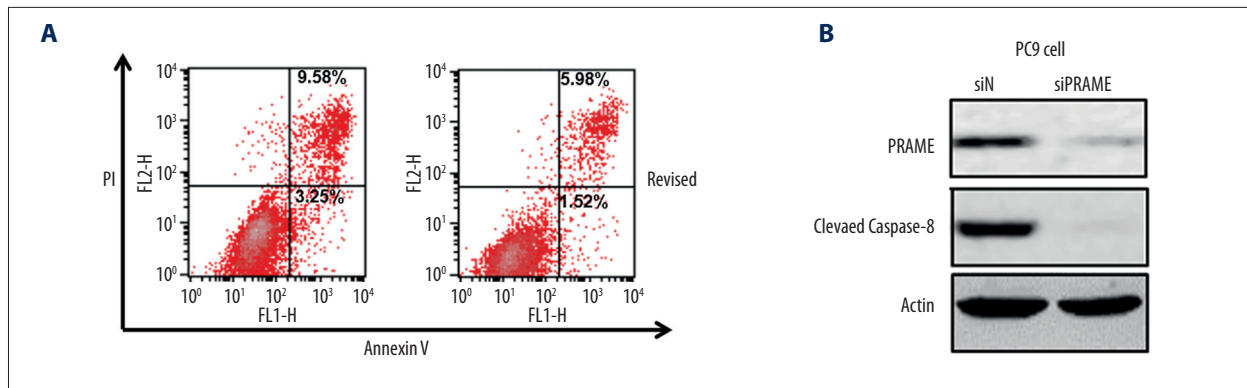


Figure 4. Cell apoptosis of PRAME siRNA-treated PC9 cells. **(A)** Flow cytometry analysis of apoptotic PC9 cells with PRAME (siPRAME) or control siRNA (siN). The lower right quadrant represents the early apoptotic cells and the upper right quadrant contains the late apoptotic cells. **(B)** The protein expression of cleaved caspase-8 detected by Western blotting. Actin serves as the loading control.

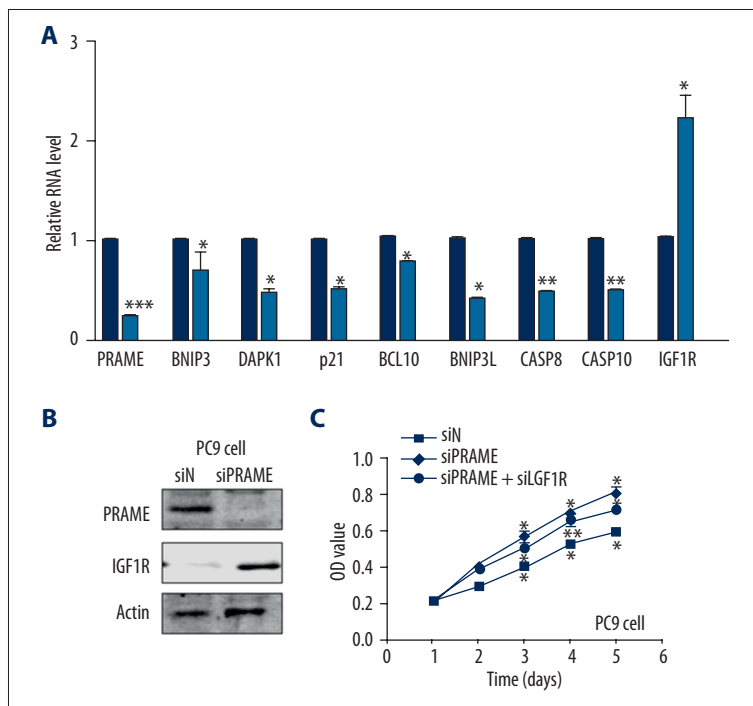


Figure 5. Genes regulated by PRAME siRNA treatment. **(A)** Gene expression in PC9 cells after PRAME knockdown was analyzed by RT-PCR. The expression levels of different genes in cells treated with PRAME siRNA (siPRAME) were normalized to that in cells treated with control siRNA (siN). **(B)** Western blot showing the expression of IGF1R in PC9 cells treated with PRAME siRNA (siPRAME). **(C)** MTT assay of PC9 cells treated with control siRNA (siN), PRAME siRNA (siPRAME), and PRAME siRNA+IGF1R siRNA (siPRAME+siIGF1R).

receptor 1 (IGF1R) are increased after PRAME siRNA treatment (Figure 5B). To examine the contribution of IGF1R to PRAME-mediated effects, we treated the cells with both PRAME siRNA and IGF1R siRNA. The result shows that PRAME siRNA-induced increase of PC9 cell proliferation is attenuated by IGF1R siRNA treatment (Figure 5C).

Discussion

PRAME has been detected mostly in cancers and PRAME expression correlates with the prognosis of cancers. Consistent with previous studies, our study also showed that PRAME was

present in normal human lung tissue and the human lung adenocarcinoma and lung cancer cell lines PC9 and A549. However, in contrast to the expression profile of PRAME in other tissues, the normal human lung tissue exhibits higher expression level in comparison with that in human lung adenocarcinoma, as evidenced by the immunohistochemical staining and RT-PCR studies. Decreased PRAME expression may promote proliferation and cancer development of lung adenocarcinoma.

It is well known that the balance of proliferation and apoptosis plays important roles in the control of tumor growth. We demonstrated that knockdown of PRAME using siRNA in these cells promoted cell proliferation and decreased apoptosis. Multiple

genes related to proliferation and apoptosis have been demonstrated to contribute to tumor cell growth. We further characterized the gene expression profiles in the lung cancer cell lines PC9 and A549 after PRAME inhibition. The Bcl-2 family of proteins is critical for the regulation of apoptosis induced by various stimuli [14]. BNIP3, a Bcl-2 family member, is a pro-apoptotic protein, which has been shown to contribute to hypoxia-induced autophagy and cell death [15]. BNIP3L is a functional homolog of BNIP3. It has been shown that BNIP3L is induced by the tumor suppressor p53 and contributes to apoptosis under hypoxia [16]. In our study, we demonstrate that inhibition of PRAME decreased the expression of BNIP3 and BNIP3L, leading to decreased apoptosis and increased proliferation of lung cancer cells. Some other genes, such as Bcl10 [17] and death-associated protein kinase 1 (DAPK1) [18], which have been shown to promote apoptosis, have also been found to be decreased in lung cancer cells after PRAME siRNA transfection. The down-regulation of 2 apoptosis-related cysteine proteases CASP8 and CASP10 in lung cancer cells treated with PRAME siRNA further supports that inhibition of PRAME leads to apoptosis inhibition. These results suggest that PRAME regulates the apoptosis of lung cancer cells by modulating the expression of these apoptosis-related genes.

The cyclin-dependent kinase (CDK) inhibitor p21 binds to several CDKs and inhibits their activities, leading to growth

arrest and cellular senescence. The expression of this gene is under the control of the tumor suppressor protein p53 [19]. Consistent with the role of p21 in cell growth, we found that PRAME knockdown suppressed the expression of p21, leading to the increased cell growth of lung cancer cell lines PC9 and A549. Several lines of evidence demonstrate that the gene expression of IGF1R contributes to cell proliferation, and cell proliferation can be inhibited by targeting IGF1R [20–22]. Consistent with these studies, we showed increased mRNA and protein expression levels of IGF1R accompanied with enhanced proliferation of lung cancer cells after PRAME knockdown. The attenuation of PRAME knockdown-induced proliferation by IGF1R siRNA transfection further supports the dependence of IGF1R in PRAME-mediated effect on lung cancer cell proliferation.

Conclusions

Our results demonstrate that PRAME regulates the apoptosis of lung cancer cells by modulating the expression of selected apoptosis-related genes. Down-regulation of PRAME promotes proliferation of lung cancer cells in an IGF1R-dependent manner, which reduces the expression of pro-apoptosis genes. PRAME-mediated effects in lung cancer cells advanced our understanding of the biological roles of PRAME in different tissues.

References:

- Ikeda H, Lethe B, Lehmann F et al: Characterization of an antigen that is recognized on a melanoma showing partial HLA loss by CTL expressing an NK inhibitory receptor. *Immunity*, 1997; 6: 199–208
- Szczepanski MJ, Whiteside TL: Elevated PRAME expression: what does this mean for treatment of head and neck squamous cell carcinoma? *Biomark Med*, 2013; 7: 575–78
- Tan P, Zou C, Yong B et al: Expression and prognostic relevance of PRAME in primary osteosarcoma. *Biochem Biophys Res Commun*, 2012; 419: 801–8
- Oberthuer A, Hero B, Spitz R et al: The tumor-associated antigen PRAME is universally expressed in high-stage neuroblastoma and associated with poor outcome. *Clin Cancer Res*, 2004; 10: 4307–13
- Epping MT, Hart AA, Glas AM et al: PRAME expression and clinical outcome of breast cancer. *Br J Cancer*, 2008; 99: 398–403
- Steinbach D, Hermann J, Viehmann S et al: Clinical implications of PRAME gene expression in childhood acute myeloid leukemia. *Cancer Genet Cytogenet*, 2002; 133: 118–23
- Oehler VG, Guthrie KA, Cummings CL et al: The preferentially expressed antigen in melanoma (PRAME) inhibits myeloid differentiation in normal hematopoietic and leukemic progenitor cells. *Blood*, 2009; 114: 3299–308
- Tanaka N, Wang YH, Shiseki M et al: Inhibition of PRAME expression causes cell cycle arrest and apoptosis in leukemic cells. *Leuk Res*, 2011; 35: 1219–25
- Epping MT, Wang L, Edell MJ et al: The human tumor antigen PRAME is a dominant repressor of retinoic acid receptor signaling. *Cell*, 2005; 122: 835–47
- De Carvalho DD, Mello BP, Pereira WO, Amarante-Mendes GP: PRAME/EZH2-mediated regulation of TRAIL: a new target for cancer therapy. *Curr Mol Med*, 2013; 13: 296–304
- Bankovic J, Stojisic J, Jovanovic D et al: Identification of genes associated with non-small-cell lung cancer promotion and progression. *Lung Cancer*, 2010; 67: 151–59
- Liu J, Cho SN, Akkanti B et al: ErbB2 pathway activation upon Smad4 loss promotes lung tumor growth and metastasis. *Cell Rep*, 2015 [Epub ahead of print]
- Liu J, Yu G, Zhao Y et al: REGgamma modulates p53 activity by regulating its cellular localization. *J Cell Sci*, 2010; 123: 4076–84
- Bonnefoy-Berard N, Aouacheria A, Verschelde C et al: Control of proliferation by Bcl-2 family members. *Biochim Biophys Acta*, 2004; 1644: 159–68
- Azad MB, Gibson SB: Role of BNIP3 in proliferation and hypoxia-induced autophagy: implications for personalized cancer therapies. *Ann NY Acad Sci*, 2010; 1210: 8–16
- Fei P, Wang W, Kim SH et al: Bnip3L is induced by p53 under hypoxia, and its knockdown promotes tumor growth. *Cancer Cell*, 2004; 6: 597–609
- Zhang Q, Siebert R, Yan M et al: Inactivating mutations and overexpression of BCL10, a caspase recruitment domain-containing gene, in MALT lymphoma with t(1;14)(p22;q32). *Nat Genet*, 1999; 22: 63–68
- Wu B, Yao H, Wang S, Xu R: DAPK1 modulates a curcumin-induced G2/M arrest and apoptosis by regulating STAT3, NF-kappaB, and caspase-3 activation. *Biochem Biophys Res Commun*, 2013; 434: 75–80
- Gartel AL, Radhakrishnan SK: Lost in transcription: p21 repression, mechanisms, and consequences. *Cancer Res*, 2015; 65: 3980–85
- Dai W, Bai Y, Hebda L et al: Calcium deficiency-induced and TRP channel-regulated IGF1R-PI3K-Akt signaling regulates abnormal epithelial cell proliferation. *Cell Death Differ*, 2014; 21: 568–81
- Jia Y, Zhang Y, Qiao C et al: IGF-1R and ErbB3/HER3 contribute to enhanced proliferation and carcinogenesis in trastuzumab-resistant ovarian cancer model. *Biochem Biophys Res Commun*, 2013; 436: 740–45
- Chen L, Wang Q, Wang GD et al: miR-16 inhibits cell proliferation by targeting IGF1R and the Raf1-MEK1/2-ERK1/2 pathway in osteosarcoma. *FEBS Lett*, 2013; 587: 1366–72